Corrected 9 January 2020. See full text.

ENHANCER GENOMICS

Brain cell type–specific enhancer–promoter interactome maps and disease-risk association

Alexi Nott[1]*, Inge R. Holtman[1,2]*, Nicole G. Coufal[3,4]*, Johannes C. M. Schlachetzki[1], Miao Yu[5], Rong Hu[5], Claudia Z. Han[1], Monique Pena[3], Jiayang Xiao[3], Yin Wu[3], Zahara Keulen[3], Martina P. Pasillas[1], Carolyn O'Connor[6], Christian K. Nickl[1], Simon T. Schafer[3], Zeyang Shen[1,7], Robert A. Rissman[8,9], James B. Brewer[8], David Gosselin[1,10], David D. Gonda[11], Michael L. Levy[11], Michael G. Rosenfeld[12], Graham McVicker[13], Fred H. Gage[3], Bing Ren[5,14], Christopher K. Glass[1,15]†

Noncoding genetic variation is a major driver of phenotypic diversity, but functional interpretation is challenging. To better understand common genetic variation associated with brain diseases, we defined noncoding regulatory regions for major cell types of the human brain. Whereas psychiatric disorders were primarily associated with variants in transcriptional enhancers and promoters in neurons, sporadic Alzheimer's disease (AD) variants were largely confined to microglia enhancers. Interactome maps connecting disease-risk variants in cell-type–specific enhancers to promoters revealed an extended microglia gene network in AD. Deletion of a microglia-specific enhancer harboring AD-risk variants ablated *BIN1* expression in microglia, but not in neurons or astrocytes. These findings revise and expand the list of genes likely to be influenced by noncoding variants in AD and suggest the probable cell types in which they function.

The central nervous system is a complex organ consisting of diverse and highly interconnected cells. Single-cell–sequencing technologies have advanced our understanding of the molecular phenotypes of human neurons, microglia, astrocytes, oligodendrocytes, and other cell types that reside within the brain (*1*–*3*), but the transcriptional mechanisms that control their developmental and functional properties in health and disease remain less well understood. Genome-wide association studies (GWASs) provide a genetic approach to identify molecular pathways involved in complex traits and diseases by defining associations between genetic variants and phenotypes of interest (*4*, *5*). Large-scale GWASs have discovered hundreds of single-nucleotide polymorphisms (SNPs) associated with the risk of neurological and psychiatric disorders. The vast majority of these disease-risk genetic variants are located in noncoding regions of the genome (*5*). The causal variants and the specific cell type(s) in which the disease-risk variants may be active is often unclear. GWAS-identified risk variants in noncoding regions of the genome can exert phenotypic effects through perturbation of transcriptional gene promoters and enhancers (*4*). Enhancers are short regions of DNA that bind transcription factors to enhance messenger RNA expression from target promoters. Clusters of multiple enhancers, referred to as super-enhancers, are particularly important in driving the expression of cell-identity genes (*6*). Enhancer repertoires underlie particular patterns of gene expression and enable cell-type–specific responses (*7*). The activity of enhancers depends on three-dimensional enhancer–promoter interactions (*8*); however, the enhancer–promoter interactome of different brain cell types in vivo remains largely unknown.

To characterize transcriptional regulatory elements within different cell types of the human brain, PU.1$^+$ microglia, NEUN$^+$ neuronal, OLIG2$^+$ oligodendrocyte, and NEUN^{neg} LHX2$^+$ astrocyte nuclei were isolated from resected cortical brain tissue from six individuals by fluorescent-activated nuclei sorting (fig. S1, A and B, and table S1). Cell-type–specific populations of 200,000 nuclei were subjected to the assay for transposase-accessible chromatin sequencing (ATAC-seq), which identifies open regions of chromatin (*9*), and cell-type–specific populations of 500,000 nuclei were subjected to H3K27ac and H3K4me3 chromatin immunoprecipitation sequencing (ChIP-seq), which predominantly identifies active chromatin regions and promoters, respectively (*10*, *11*). These datasets clustered according to cell type of origin and exhibited cell-type–specific patterns (Fig. 1A and fig. S1, C to E). Promoter H3K27ac signal correlated with gene expression of the corresponding cell type more closely than ATAC-seq and H3K4me3 ChIP-seq (fig. S1F) (*12*). Promoters associated with cell-type signature genes preferentially exhibited corresponding H3K27ac profiles (fig. S1G) (*13*). Oligodendrocyte nuclei contain a low signal for oligodendrocyte precursor cell signature genes, whereas neuronal nuclei represent a mixture of excitatory and inhibitory subtypes (fig. S1G). ATAC-seq and H3K27ac ChIP-seq profiles generated from PU.1 nuclei were highly correlated with those previously defined in ex vivo microglia (fig. S1, C and D) (*14*). Promoter H3K27ac signal was increased at microglia signature genes compared with genes associated with other myeloid populations (fig. S1H) (*15*). Cell-type–specific promoter activity defined by differential H3K27ac mirrored cell-type patterns of gene expression (*12*), as well as ATAC-seq and H3K4me3 enrichment, and were associated with gene ontologies representative of each cell type (fig. S2, A to D, and table S2).

We identified putative active promoters and enhancers in each cell type and found a one-to-many relationship between promoters and enhancers (*8*). Whereas active promoters are largely shared between cell types (Fig. 1B), a relatively small fraction of active enhancers overlap between cell types (Fig. 1C), indicating that cell-type specificity is mainly captured within the enhancer repertoire. Most bulk brain-enhancer regions identified by PsychENCODE overlapped with the nuclei cell-type enhancers (94%) (*13*). However, analysis of cell-specific nuclei expanded the total number of putative brain enhancers by 87%.

To determine the enrichment of genetic variants associated with complex traits and diseases in cell-type–specific regulatory regions, we performed linkage disequilibrium score (LDSC) regression analysis of heritability (*16*). LDSC uses GWAS summary statistics to determine whether genetic heritability for a trait or disease is enriched for SNPs within genome annotations while accounting for linkage disequilibrium. We obtained GWAS summary statistics for neurological and psychiatric disorders and neurobehavior traits (*17*) (table S3). We found a strong enrichment of heritability for variants within neuronal

[1]Department of Cellular and Molecular Medicine, University of California, San Diego, La Jolla, CA 92093, USA. [2]Section Molecular Neurobiology, Department of Biomedical Sciences of Cells & Systems, University Medical Center Groningen, University of Groningen, 9713 AV Groningen, the Netherlands. [3]Laboratory of Genetics, The Salk Institute for Biological Studies, La Jolla, CA 92037, USA. [4]Department of Pediatrics, University of California, San Diego, La Jolla, CA 92093, USA. [5]Ludwig Institute for Cancer Research, La Jolla, CA 92093, USA. [6]Flow Cytometry Core Facility, The Salk Institute for Biological Studies, La Jolla, CA 92037, USA. [7]Department of Bioengineering, University of California, San Diego, La Jolla, CA 92093, USA. [8]Department of Neurosciences, University of California, San Diego, La Jolla, CA 92093, USA. [9]Veterans Affairs San Diego Healthcare System, San Diego, CA 92161, USA. [10]Centre de Recherche du Centre Hospitalier Universitaire de Québec–Université Laval, Département de Médecine Moléculaire, Faculté de Médecine, Université Laval, Québec G1V 4G2, Canada. [11]Department of Neurosurgery, University of California, San Diego–Rady Children's Hospital, San Diego, CA 92123, USA. [12]Howard Hughes Medical Institute, Department and School of Medicine, University of California, San Diego, La Jolla, CA 92093, USA. [13]The Salk Institute for Biological Studies, La Jolla, CA 92037, USA. [14]Department of Cellular and Molecular Medicine, Center for Epigenomics, University of California, San Diego, School of Medicine, La Jolla, CA 92093, USA. [15]Department of Medicine, University of California, San Diego, La Jolla, CA 92093, USA.
*These authors contributed equally to this work.
†Corresponding author. Email: ckg@ucsd.edu

Corrected 9 January 2020. See full text.

enhancers and promoters for all psychiatric disorders and behavioral traits (Fig. 1D), which was substantially lower in PsychENCODE bulk brain enhancers (Fig. 1D) (*13*). By contrast, AD SNP heritability was most highly enriched in microglia-regulatory elements (Fig. 1D), specifically microglia enhancers (*18*–*23*).

De novo motif analyses at open chromatin within enhancers identified transcription factor–binding motifs associated with each cell type (fig. S3). In addition, H3K27ac-defined active promoters identified 288 human transcription factors that were active in a cell-type–specific manner (fig. S4 and table S2) (*24*), several of which have been associated with disease (fig. S5 and table S4). Integrating cell-type–specific transcription factors with enhancer motifs of the corresponding cell type identifies major drivers of cell ontogeny.

The relationship between promoters and distal regulatory regions for different cell types in the brain is largely unknown. We used proximity ligation-assisted ChIP-seq (PLAC-seq), in which proximity ligation preceded an enrichment for active promoters by H3K4me3 ChIP-seq (*25*). Chromatin loops were identified between active promoters and distal regulatory regions in microglia, neurons, and oligodendrocytes (*26*). An example is the *SALL1* locus, which has interactions with cell-type–specific enhancers, including chromatin loops to a microglia-specific super-enhancer (Fig. 2A). There were 219,509 significant interactions across cell types, and replicates clustered according to origin (fig. S6, A and B, and table S5). A strong H3K4me3 signal did not dictate that an interaction would occur (fig. S6C), suggesting that PLAC-seq captures a unique dimension of the chromatin conformation.

A subset of chromatin interactions was significantly more active in each cell type and colocalized with increased ATAC-seq, H3K27ac, and H3K4me3 ChIP-seq signal in a cell-type–specific manner (Fig. 2B and fig. S6D). Active

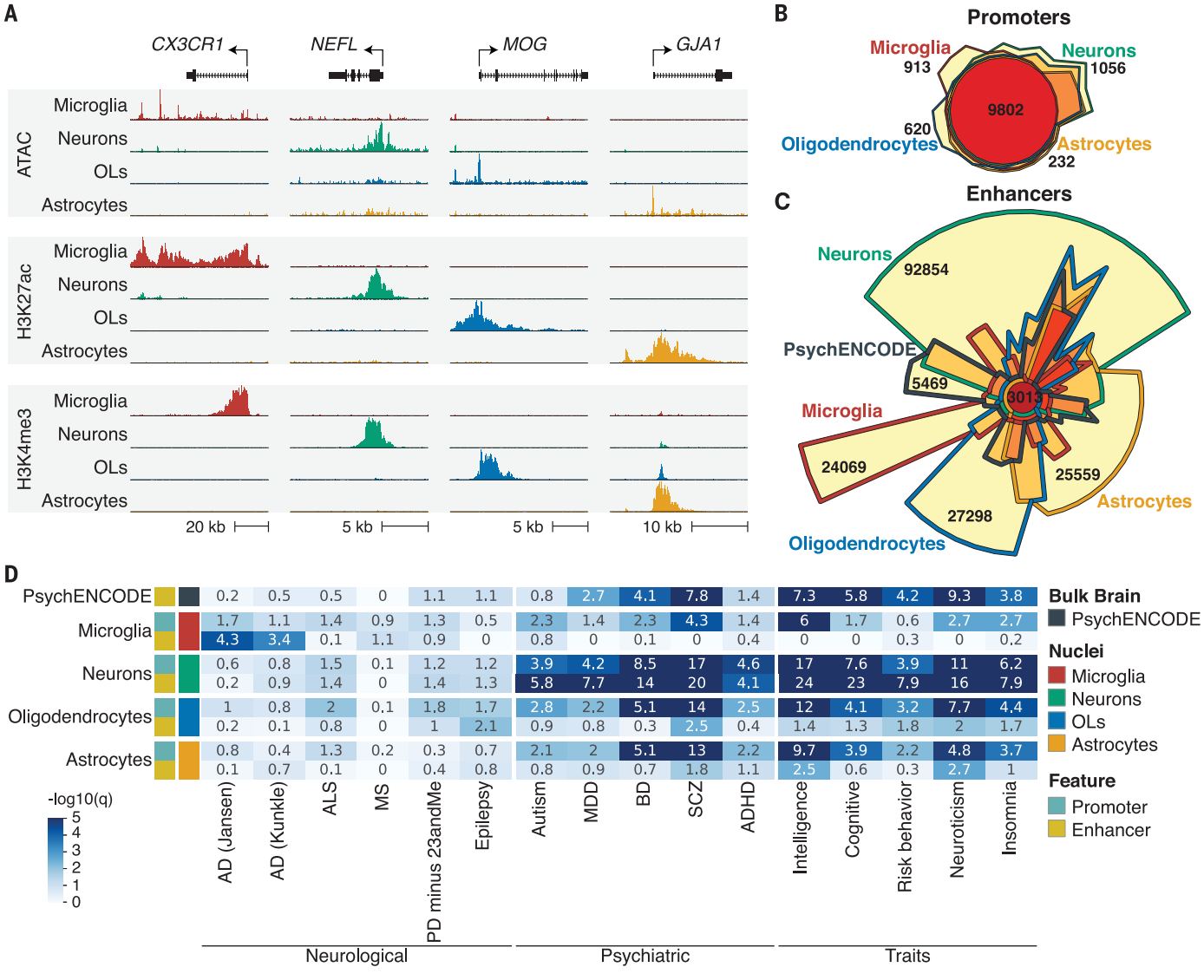

Fig. 1. Cell-type–specific genomic regulatory region enrichments for GWAS risk variants for brain disorders and behavioral traits. (**A**) UCSC genome browser visualization of ATAC-seq (top panel), H3K4me3 ChIP-seq (middle panel), and H3K27ac ChIP-seq (bottom panel) for brain nuclei populations. Shown is a representative gene for microglia (*CX3CR1*), neurons (*NEFL*), oligodendrocytes (*MOG*), and astrocytes (*GJA1*). (**B**) Chow–Ruskey plot of promoter regions defined for cell populations. (**C**) Chow–Ruskey plot of enhancer regions defined for cell populations and PsychENCODE enhancers defined using bulk brain. (**D**) Heatmap of LDSC analysis for genetic variants associated with brain disorders and behavior traits displayed as −log10(q) value for significance of enrichment for promoter and enhancer regions of cell populations and PsychENCODE bulk brain enhancers. OL, oligodendrocytes.

Corrected 9 January 2020. See full text.

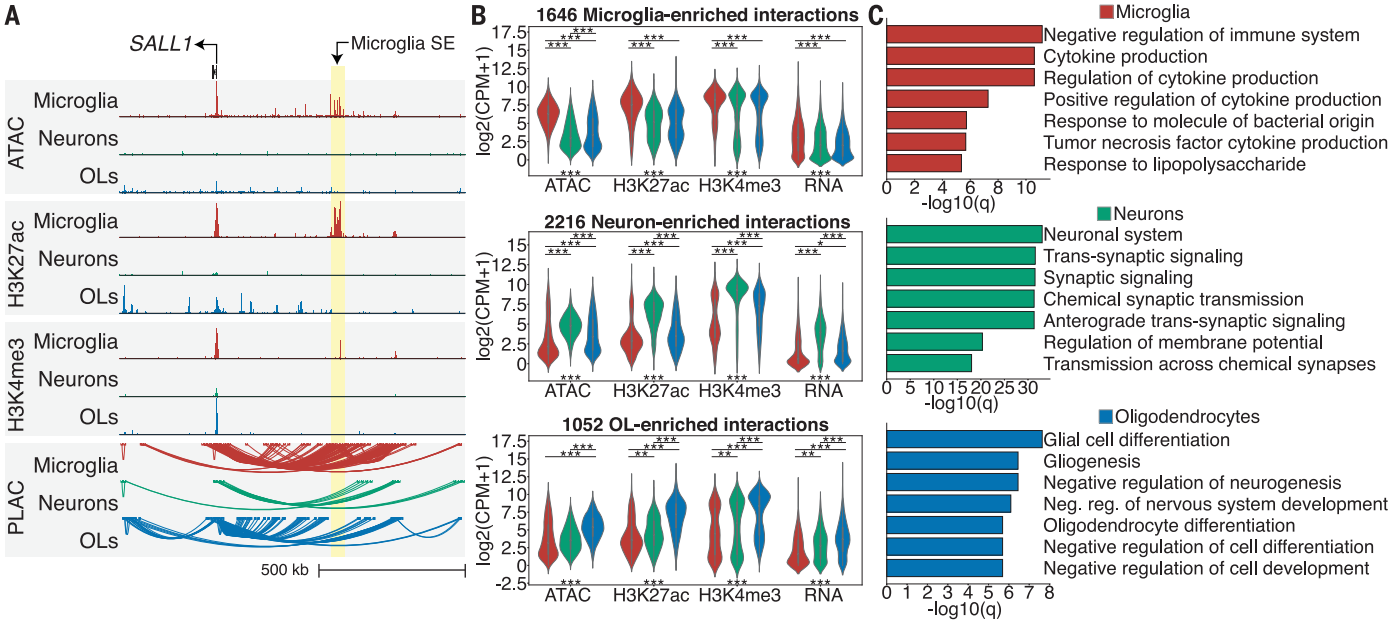

Fig. 2. Chromatin loops link promoters to active gene-regulatory regions. (**A**) UCSC genome browser visualization of ATAC-seq, H3K27ac ChIP-seq, H3K4me3 ChIP-seq and PLAC-seq loops at the *SALL1* locus. The microglia-specific super-enhancer is associated with microglia interactions (highlighted yellow). (**B**) Violin plots of ATAC-seq, H3K27ac ChIP-seq, H3K4me3 ChIP-seq and RNA-seq $\log_2$(CPM+1) values at PLAC-seq up-regulated interactions shown in fig. S6D for microglia, neurons, and oligodendrocytes; ***p < 1e-12; **p < 1e-5; *p < 1e-3 by Kruskal–Wallis between-groups test. (**C**) Metascape enrichment analyses of active genes identified at PLAC-seq up-regulated interactions shown in fig. S6D for microglia, neurons, and oligodendrocytes shown as −log10(q) values.

promoters linked to microglia-, neuron-, and oligodendrocyte-enriched interactions were associated with gene ontology terms representative of each cell type, supporting the ability of the PLAC interactome to annotate cell-type–specific promoter–enhancer interactions (Fig. 2C).

We identified 2,954 super-enhancers in microglia, neurons, and oligodendrocytes, of which 83% had PLAC interactions and were linked to promoters with elevated H3K27ac levels compared with promoters linked to regular enhancers (fig. S7, A and B). Many super-enhancers harbored GWAS disease-risk variants and were connected to cell-type–specific genes, suggesting that a subset of GWAS variants act on super-enhancers to affect gene expression (fig. S7A and table S6).

To better understand AD genetics and the microglia interactome, we distinguished likely causal variants from those in linkage disequilibrium by applying fine mapping and identified 261 credible set variants (*18*). In many instances, such as the *BIN1*, *PICALM*, and *SORL1* loci, the fine-mapped variants overlapped with microglia-specific enhancers that were PLAC linked to corresponding gene promoters (Fig. 3A). Next, we determined PLAC interactions between active promoters and AD-risk–credible set variants (*19*) and identified 41 genes that were linked to these variants across cell types (fig. S8). Twenty-five of the PLAC-linked AD-risk genes were identified in microglia, of which 14 were not detected in the other cell types (Fig. 3B and fig. S8). A broader set of 134 putative risk genes were identified by applying the same analysis to all genome-wide significant variants found in two AD GWASs (figs. S8 and S9, A and B, and table S7) (*18*, *19*).

Protein–protein interaction (PPI) network analysis showed that microglia AD-risk genes identified by PLAC-seq were highly connected with GWAS-assigned genes and centered around *APOE*, whereas PPI networks for neurons and oligodendrocytes were smaller in scope (fig. S9, C to E). Microglia AD-assigned genes were associated with gene ontology terms for immune function, whereas gene ontology terms for amyloid-beta processing were associated with neurons, microglia, and oligodendrocytes (fig. S9F).

PLAC interactions altered the interpretation of AD-risk variants for three reasons. First, we found AD-risk variants that were linked to more distal active promoters and not the closest gene promoter. An example is the *SLC24A4* locus, which had AD-risk variants that were connected to the proximal active promoters of *ATXN3*, *TRIP11*, and *CPSF2*, but not to *SLC24A4* (Fig. 3C). Second, we observed enhancers harboring AD-risk variants that were PLAC linked to active promoters of both GWAS-assigned genes and an extended subset of genes not assigned to GWAS loci. An example is the *CLU* locus, which had PLAC-linked AD-risk variants to the GWAS-assigned genes *CLU* and *PTK2B* and an extended set of genes: *TRIM35*, *CHRNA2*, *SCARA3*, and *CCDC25* (Fig. 3D). Finally, we identified cell-type–specific enhancers harboring AD-risk variants that were linked to genes expressed in multiple cell types, implicating cell-type–specific disease susceptibility. Examples are the *PICALM* and *BIN1* loci, which, despite being expressed in multiple cell types (*12*), had microglia-specific enhancers harboring AD-risk variants (Figs. 3E and 4A).

The *BIN1* microglia-specific enhancer is PLAC linked to the *BIN1* promoter (Fig. 4A), binds to PU.1 (*14*), and contains the AD-risk variant rs6733839, which has the second-highest AD-risk score after *APOE* and was fine mapped as a casual variant (Fig. 3A). Functionality of this microglia-specific enhancer was validated by CRISPR/Cas9-mediated deletion of a 363-bp region in two human pluripotent stem cell (PSC) lines (fig. S10, A to C). PSC control ($BIN1^{control}$) and *BIN1* enhancer deletion ($BIN1^{enh\_del}$) lines had normal karyotypes (fig. S10D) and were differentiated into microglia, neurons, and astrocytes (Fig. 4B and figs. S11, A to D, and S12, A and B). Gene-expression analysis of $BIN1^{control}$ and $BIN1^{enh\_del}$ lines in PSC and PSC-derived microglia, neurons, and astrocytes showed high correlation between samples, with clustering according to cell type (fig. S12, C and D). However, gene expression of *BIN1* was nearly absent in the $BIN1^{enh\_del}$ PSC-derived microglia, whereas *BIN1* expression in $BIN1^{enh\_del}$ PSCs and PSC-derived neurons and astrocytes was equivalent to that in

Corrected 9 January 2020. See full text.

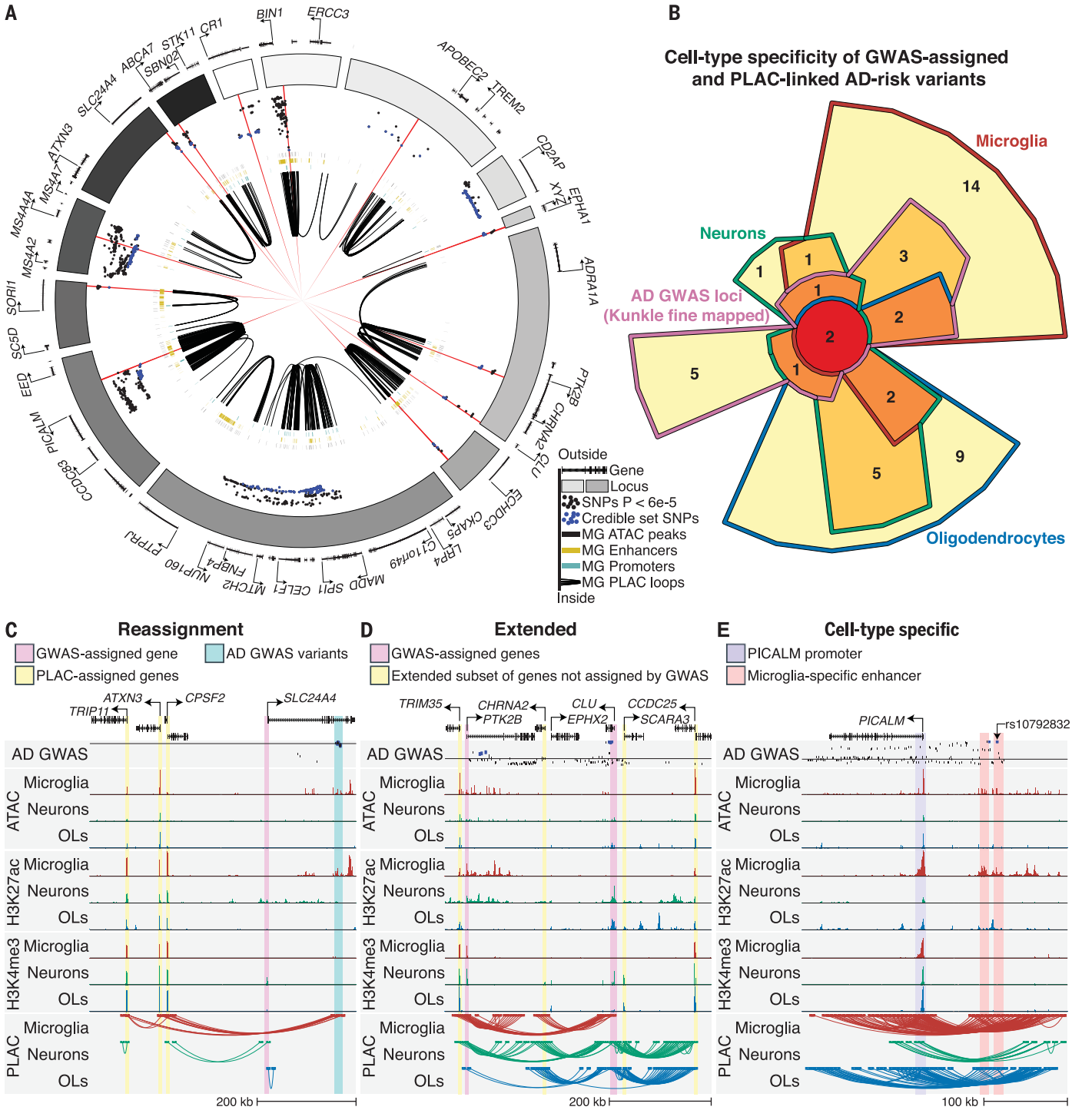

Fig. 3. Expanded gene network of AD-risk loci. (**A**) Circos plot of AD GWAS loci showing microglia enhancers (gold bars), promoters (turquoise), open chromatin regions (black bars), and PLAC-seq interactions (black loops). Dots show *z*-score values of high-confidence AD variants identified by fine mapping (Kunkle stage 1) with a log10 *p*-value < 6e-5 (*18*). Blue dots represent *z*-score values of the credible set of AD SNPs (95% confidence); red lines show 15 high-confidence AD SNPs with a posterior probability > 0.2. (**B**) Chow–Ruskey plot of genes that are GWAS assigned and PLAC-seq linked to AD-risk–credible set variants in microglia, neurons, and oligodendrocytes. (**C** to **E**) UCSC genome browser visualization of interactions at AD-risk loci demonstrating: (C) reassignment of GWAS-assigned genes, (D) extension of GWAS-assigned genes, and (E) cell-type–specific gene-regulatory regions. The AD GWAS track shows meta-analysis *p*-values of stage 2 variants (*18*); line indicates *p* = 5e-8; blue dots are fine-mapped 95% credible set variants.

Corrected 9 January 2020. See full text.

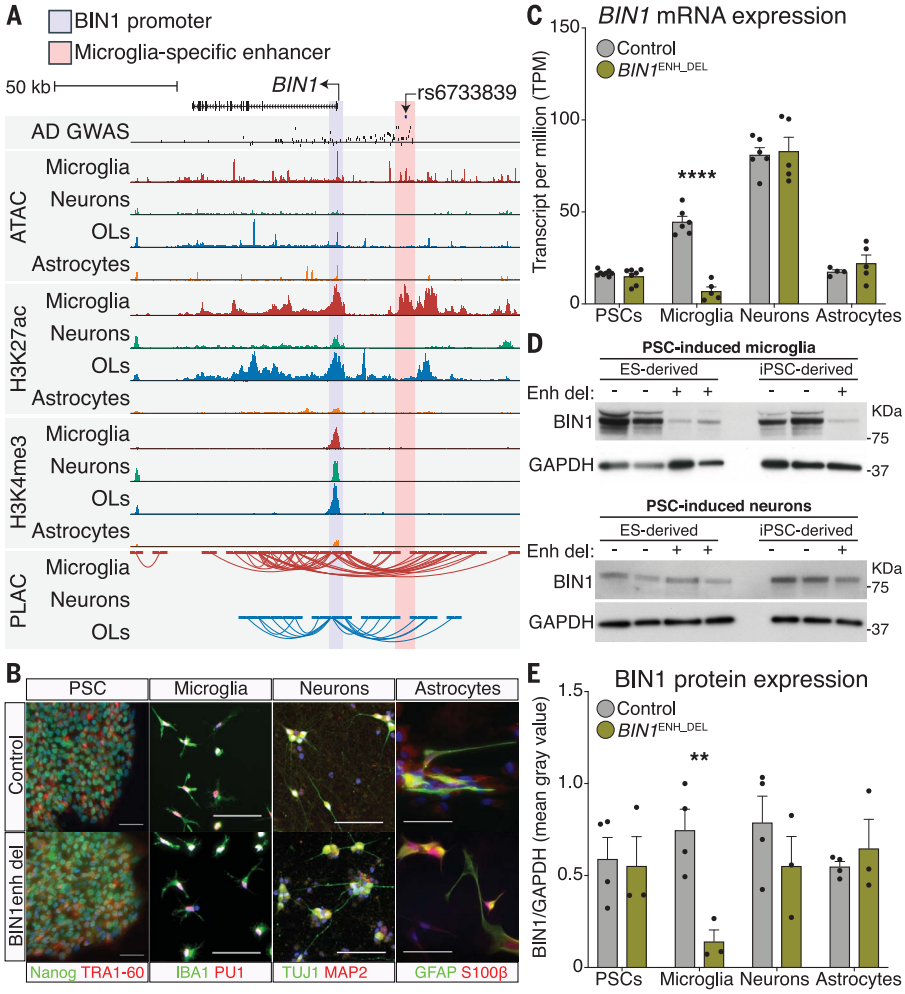

Fig. 4. Deletion of a microglia-specific enhancer harboring a lead AD-risk variant affects microglia BIN1 expression. (**A**) UCSC genome browser visualization of the *BIN1* locus showing AD-risk variants, ATAC-seq, H3K27ac ChIP-seq, H3K4me3 ChIP-seq, and PLAC-seq in different brain cell types. The shared active promoter region is highlighted in light blue; the microglia-specific enhancer region is highlighted in pink. The AD GWAS track shows meta-analysis *p*-values of stage 2 variants (*18*); line indicates *p*-value = 5e-8; blue dots are fine-mapped 95% credible set variants. (**B**) Immunohistochemistry of PSCs, microglia, neurons, and astrocytes in control and *BIN1*$^{enh\_del}$ lines stained for the indicated cell lineage markers. (**C**) *BIN1* gene expression in control and *BIN1*$^{enh\_del}$ PSCs (N = 8,7), microglia (N = 6,5), neurons (N = 6,5), and astrocytes (N = 4,5) as RNA-seq TPM. ****p < 0.0001, Benjamini–Hochberg adjusted. (**D**) Western blot of BIN1 and GAPDH in control and *BIN1*$^{enh\_del}$ PSC-derived microglia (top) and neurons (bottom). (**E**) Protein expression of BIN1 in control and *BIN1*$^{enh\_del}$ PSCs, microglia, neurons, and astrocytes determined as Western blot BIN1/GAPDH mean gray intensity. N = 4 controls, 3 *BIN1*$^{enh\_del}$ per cell type. **p < 0.01 by unpaired two-tailed t test.

BIN1^{control} cells (Fig. 4C, fig. S12E, and table S8). Western blot confirmed BIN1 protein in *BIN1*^{control} PSCs and PSC-derived microglia, neurons, and astrocytes (Fig. 4, D and E, and fig. S12F). BIN1 expression was unchanged in *BIN1*$^{enh\_del}$ PSC-derived microglia precursor hematopoietic stem cells, indicating that microglia derivation was unaffected (fig. S12F). However, BIN1 was substantially reduced in *BIN1*$^{enh\_del}$ microglia and not in neurons and astrocytes (Fig. 4, D and E). This finding that the most significant GWAS risk allele associated with *BIN1* resides in a microglia-specific enhancer provides a rationale for further investigation of its function in these cells (*27*).

The present study provides evidence that the identification of cell-type–specific promoter–enhancer interactomes enables substantial advances in the interpretation of GWAS-risk alleles and establishes a new resource for this purpose in a broad spectrum of neurological and psychiatric diseases. Major goals will be to extend these approaches to diseased tissues and to refine nuclear-sorting protocols to interrogate enhancer landscapes of informative cell subsets such as amyloid plaque–associated microglia (*28*). Disease-specific regulatory elements are likely to be influenced by genetic variation, which, because of our limited sample size, may partly explain the lack of overlap of a subset of risk alleles with the current regulatory atlases. The acquisition of more samples will provide further opportunity to evaluate inter-individual variation on enhancer selection and function. We expect that these approaches will provide qualitatively new insights into disease mechanisms that may be of value in developing new approaches for prevention and treatment.

REFERENCES AND NOTES

1. B. B. Lake *et al.*, *Science* **352**, 1586–1590 (2016).
2. B. B. Lake *et al.*, *Nat. Biotechnol.* **36**, 70–80 (2018).
3. H. Mathys *et al.*, *Nature* **570**, 332–337 (2019).
4. M. D. Gallagher, A. S. Chen-Plotkin, *Am. J. Hum. Genet.* **102**, 717–730 (2018).
5. M. T. Maurano *et al.*, *Science* **337**, 1190–1195 (2012).
6. D. Hnisz *et al.*, *Cell* **155**, 934–947 (2013).
7. S. Heinz, C. E. Romanoski, C. Benner, C. K. Glass, *Nat. Rev. Mol. Cell Biol.* **16**, 144–154 (2015).
8. M. R. Mumbach *et al.*, *Nat. Methods* **13**, 919–922 (2016).
9. X. Chen *et al.*, *Nat. Methods* **13**, 1013–1020 (2016).
10. M. P. Creyghton *et al.*, *Proc. Natl. Acad. Sci. U.S.A.* **107**, 21931–21936 (2010).
11. N. D. Heintzman *et al.*, *Nat. Genet.* **39**, 311–318 (2007).
12. Y. Zhang *et al.*, *Neuron* **89**, 37–53 (2016).
13. D. Wang *et al.*, *Science* **362**, eaat8464 (2018).
14. D. Gosselin *et al.*, *Science* **356**, eaal3222 (2017).
15. M. J. C. Jordão *et al.*, *Science* **363**, eaat7554 (2019).
16. B. Bulik-Sullivan *et al.*, *Nat. Genet.* **47**, 1236–1241 (2015).
17. Materials and methods are available as supplementary materials.
18. B. W. Kunkle *et al.*, *Nat. Genet.* **51**, 414–430 (2019).
19. I. E. Jansen *et al.*, *Nat. Genet.* **51**, 404–413 (2019).
20. K. L. Huang *et al.*, *Nat. Neurosci.* **20**, 1052–1061 (2017).
21. G. Novikova, G. Novikova, M. Kapoor, J. TCW, E. M. Abud, A. G. Efthymiou, H. Cheng, J. F. Fullard, J. Bendl, P. Roussos, W. W. Poon, K. Hao, E. Marcora, A. M. Goate, Integration of Alzheimer's disease genetics and myeloid cell genomics identifies novel causal variants, regulatory elements, genes and pathways. bioRxiv 694281 [Preprint]. 6 July 2019. https://www.biorxiv.org/content/10.1101/694281v1.
22. K. E. Tansey, M. J. Hill, *Transl. Psychiatry* **8**, 7 (2018).
23. K. E. Tansey, D. Cameron, M. J. Hill, *Genome Med.* **10**, 14 (2018).
24. S. A. Lambert *et al.*, *Cell* **175**, 598–599 (2018).
25. R. Fang *et al.*, *Cell Res.* **26**, 1345–1348 (2016).
26. I. Juric *et al.*, *PLOS Comput. Biol.* **15**, e1006982 (2019).
27. A. Crotti *et al.*, *Sci. Rep.* **9**, 9477 (2019).
28. H. Keren-Shaul *et al.*, *Cell* **169**, 1276–1290.e17 (2017).

ACKNOWLEDGMENTS

We thank J. Collier for technical assistance, L. Van Ael for manuscript preparation, D. Skola and M. L. Gage for manuscript editing, and M. Gymrek and S. Konermann for scientific discussions. **Funding:** Support was provided by NIH grant nos. NS096170, RF1 AG061060-01, R01 AG056511-01A1, and R01 AG057706-01; the Cure Alzheimer's Fund Gifford Neuroinflammation Consortium; and UCSD Shiley-Marcos ADRC grant no. 1P30AG062429. A.N. was supported by the Alzheimer's Association (grant no. AARF-18-531498) and the Altman Clinical & Translational Research

Institute at UCSD (National Center for Advancing Translational Sciences, supported by NIH grant no. KL2TR001444). I.R.H. was supported by the VENI research program, which is financed by the Netherlands Organization for Scientific Research. N.G.C. was supported by NIH grant no. K08 NS109200-01 and The Hartwell Foundation. C.Z.H. was supported by the Cancer Research Institute Irvington Postdoctoral Fellowship Program. C.O. was funded by NIHNCI CCSG grant nos. P30 014195 and S10-OD023689. Salk facilities are supported by the Salk Cancer Center (NCI grant no. P30-CA014195). F.H.G. was supported by the JPB Foundation, the Engman Foundation, an AHA-Allen Initiative in Brain Health and Cognitive Impairment award made jointly through the American Heart Association and The Paul G. Allen Frontiers Group: 19PABH134610000, and the Dolby Foundation. J.B.B. and R.A.R. were supported by the UCSD Shiley-Marcos ADRC grant no. AG062429-01. Sequencing was conducted at the IGM Genomics Center, UCSD; the center was supported by grant nos. P30DK063491 and P30CA023100. **Author contributions:** A.N., N.G.C., J.C.M.S., and C.K.G. conceived the study. N.G.C. coordinated tissue acquisition. D.D.G. and M.L.L. resected brain tissue. A.N., C.K.N., M.P.P., and D.G. isolated nuclei and cells. N.G.C., M.P., J.X., Y.W., Z.K., and C.O. performed PSC experiments. A.N., M.Y., and R.H. prepared sequencing libraries. I.R.H., A.N., and Z.S. analyzed datasets. A.N., I.R.H., and C.K.G. wrote the manuscript with contributions from N.G.C., C.Z.H., J.C.M.S., M.G.R., F.H.G., and B.R. **Competing interests:** B.R. is a cofounder of Arima Genomics, Inc., which sells Hi-C and PLAC-seq kits. **Data and materials availability**: Data are available on dbGap (https://www.ncbi.nlm.nih.gov/projects/gap/cgi-bin/study.cgi?study_id=phs001373.v2.p2). The UCSC genome browser session (hg19) containing the processed ATAC-seq, ChIP-seq, and PLAC-seq datasets for each brain cell type is available at: https://genome.ucsc.edu/s/nottalexi/glassLab_BrainCellTypes_hg19.

SUPPLEMENTARY MATERIALS

science.sciencemag.org/content/366/6469/1134/suppl/DC1
Materials and Methods
Figs. S1 and S2
Captions for Tables S1 to S8
References (*29*–*66*)
Tables S1 to S8

View/request a protocol for this paper from *Bio-protocol*.

27 May 2019; accepted 30 October 2019
10.1126/science.aay0793

Science

Brain cell type–specific enhancer–promoter interactome maps and disease-risk association

Alexi Nott, Inge R. Holtman, Nicole G. Coufal, Johannes C. M. Schlachetzki, Miao Yu, Rong Hu, Claudia Z. Han, Monique Pena, Jiayang Xiao, Yin Wu, Zahara Keulen, Martina P. Pasillas, Carolyn O'Connor, Christian K. Nickl, Simon T. Schafer, Zeyang Shen, Robert A. Rissman, James B. Brewer, David Gosselin, David D. Gonda, Michael L. Levy, Michael G. Rosenfeld, Graham McVicker, Fred H. Gage, Bing Ren and Christopher K. Glass

Science **366** (6469), 1134-1139.
DOI: 10.1126/science.aay0793originally published online November 14, 2019

Linking enhancers to disease

Enhancers are genomic regions that regulate gene expression, sometimes in a cell-dependent manner. However, most of our knowledge of human brain cell–type enhancers derives from studies of bulk human brain tissue. Nott *et al.* examined chromatin and promoter activity in cell nuclei isolated from human brains. Genetic variants associated with brain traits and disease showed cell-specific patterns of enhancer enrichment. These data indicate that Alzheimer's disease is regulated by genetic variants within microglial cells, whereas psychiatric diseases tend to affect neurons.

Science, this issue p. 1134

Science (print ISSN 0036-8075; online ISSN 1095-9203) is published by the American Association for the Advancement of Science, 1200 New York Avenue NW, Washington, DC 20005. The title *Science* is a registered trademark of AAAS.